Stem Cell Reports, Volume *5*

Supplemental Information

Neural Stem Cells Rescue Cognitive and Motor Dysfunction in a Transgenic Model of Dementia with Lewy Bodies through a BDNF-Dependent Mechanism

Natalie R.S. Goldberg, Jacqueline Caesar, Ashley Park, Shawn Sedgh, Gilana Finogenov, Eliezer Masliah, Joy Davis, and Mathew Blurton-Jones

SUPPLEMENTAL FIGURES, LEGENDS & REFERENCES

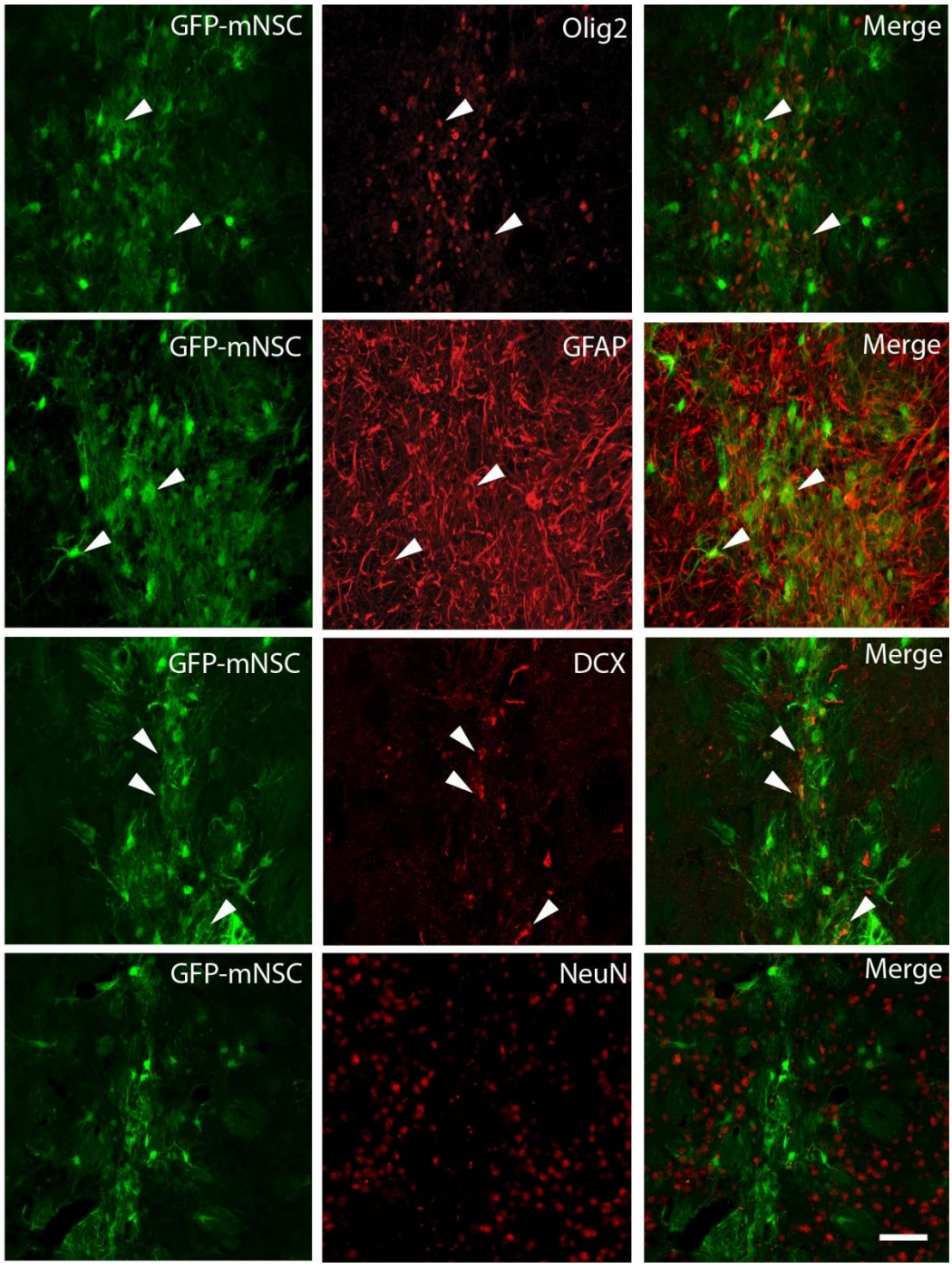

SI Figure 1. Transplanted GFP-NSCs survive and differentiate after 6 weeks, Related to Figure 1. Low-magnification confocal images demonstrate that GFP-NSCs can adopt early oligodendrocytic (Olig2), glial (GFAP) or neuronal (DCX) phenotypes, but do not yet express a more mature neuronal marker (NeuN). Scalebar=50 μm.

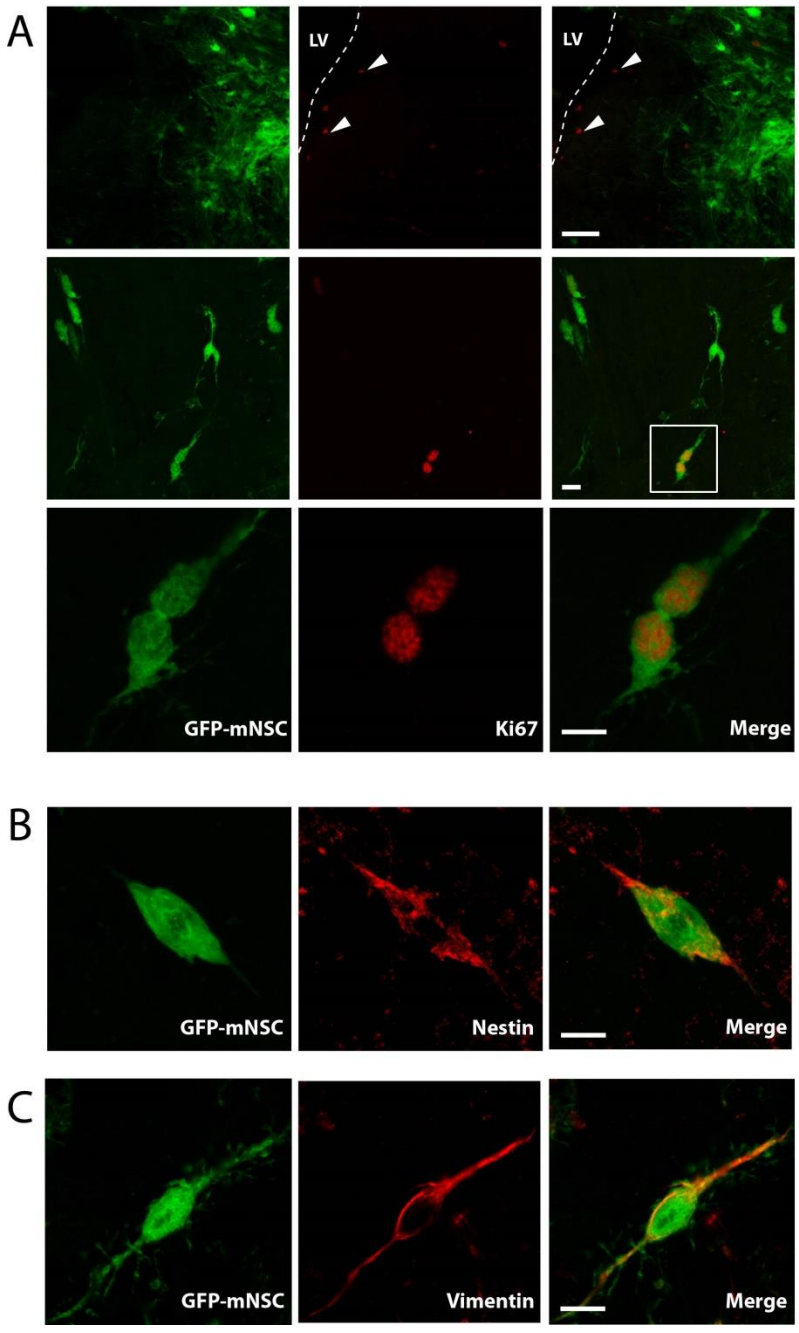

SI Figure 2. Transplanted GFP-NSCs that express markers of multipotency and proliferation are infrequent and distal to the injection site, Related to Figure 1. Endogenous cells near the lateral ventricle (LV) express the proliferation marker Ki67, but GFP-NSCs in the dorsal striatum do not (**A**). However rare examples of GFP cells that express the mitotic marker Ki67 are observed in areas that are distal to the injection site a (**A**; Scalebar=100 μm, 20 μm, 10 μm). Distally migrating NSCs also occasionally express Nestin (**B**) or Vimentin (**C**)**.** Scalebar=10 μm B,C.

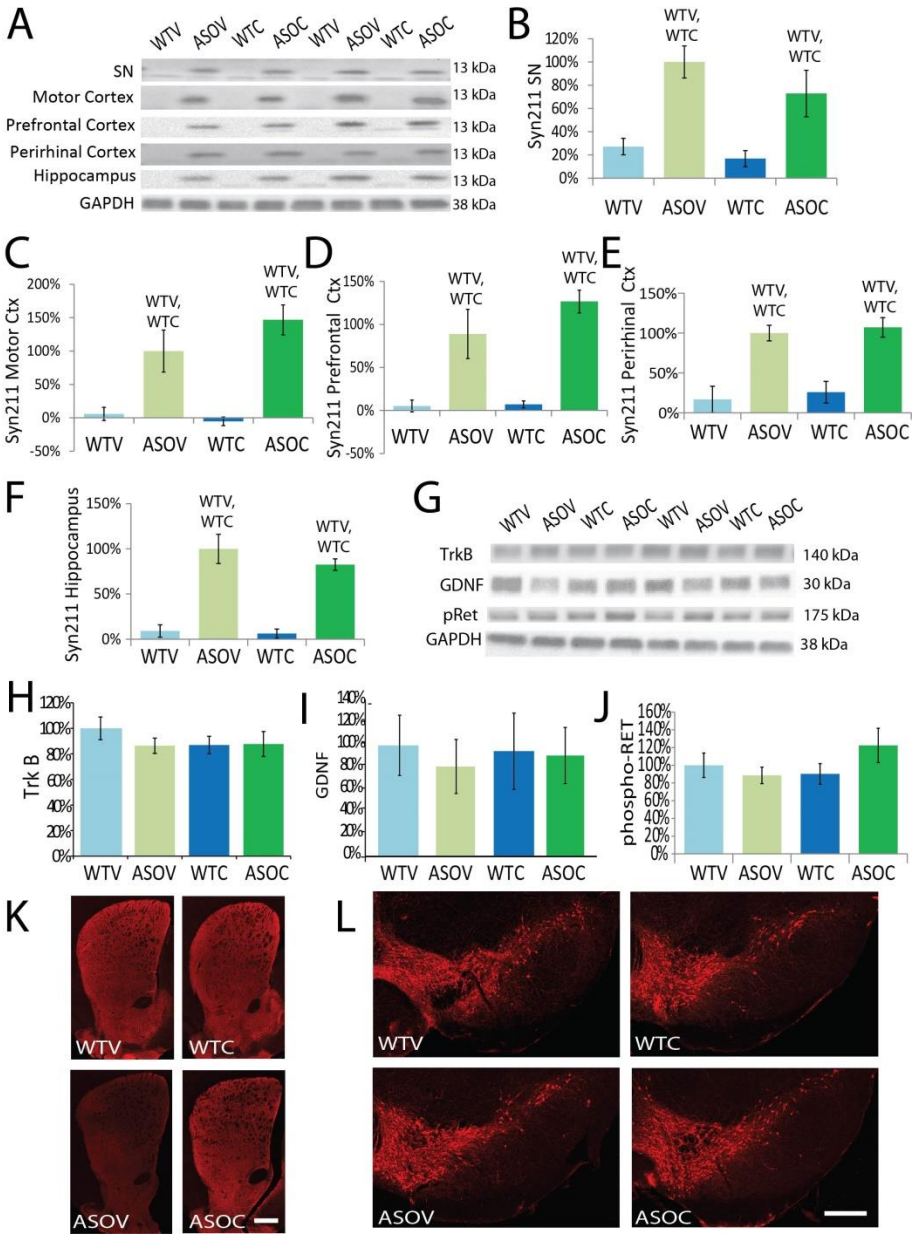

SI Figure 3. Effects of NSC transplantation on α-synuclein, neurotrophins, and tyrosine hydroxylase, Related to Figure 2. Western blot analysis of h-α-syn (Syn211) in 5 microdissected brain regions was not significantly altered by NSCs, as normalized to region-specific GAPDH (**A-F;** representative SN GAPDH shown). Complementary to NSC-induced BDNF expression in the striatum, expression its receptor TrkB was unaltered by genotype or treatment **(G,H)**. Neither GDNF nor its activated receptor phospho-RET, commonly associated with changes in DA regulation, were affected by genotype or treatment **(G,I,J)**. Representative images of TH demonstrate striatal downregulation due to h-α-syn (**K**), and confirm no loss of SNpc DA cells (**L**). Data are represented as mean ± S.E.M. All Western blot graphs are represented as % of the ASOV group. Fisher's PLSD post hoc $^{WTV,WTC}p<0.0001$.

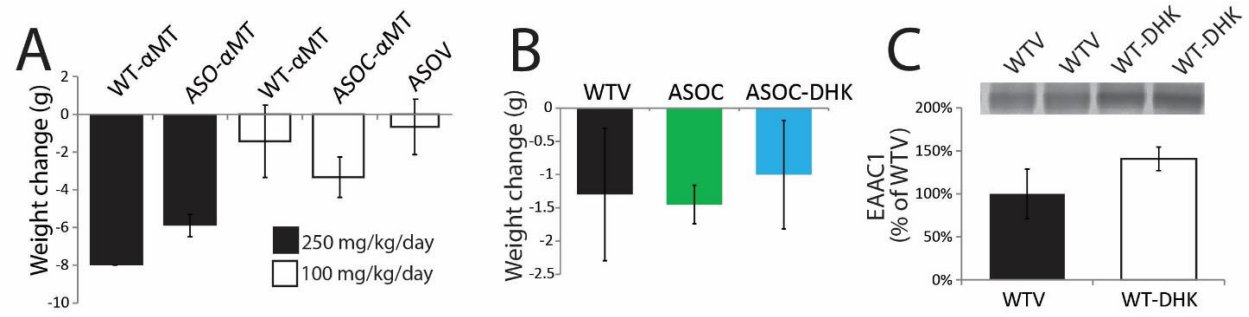

SI Figure 4. Safety and dose-response experiments for pharmacological studies, Related to Figure 4. Prior to experiments, dose response studies determined safe and optimal doses of the TH inhibitor α-methyl-p-tyrosine (αMT,100 mg/kg in 0.9% NaCl) (**A**). In addition, the safe dose of GLT-1 inhibitor dihydrokainic acid (DHK,10 mg/kg in 0.01 M PBS) was determined based on lack of weight change (**B**). The appropriate DHK dose resulted in a significant compensatory change in expression of the glutamate EAAC1 transporter (**C)**.

SI Methods

Animals. All procedures were performed in strict accordance with the University of California, Irvine animal use regulations and the NIH guide for the Care and Use of Laboratory Animals. ASO mice have been previously characterized, and are maintained on a purebred C57B6/J background by breeding heterozygous ASO mice with wild-type C57B6/J mice (Masliah, Rockenstein et al. 2000, Amschl, Neddens et al. 2013). All mice were housed on a 12 h light/dark schedule with *ad libitum* access to food and water.

Neural Stem Cell and AAV Preparation, and Stereotactic Surgery. Mouse NSCs: Hippocampal/cortical GFP-mNSCs were microdissected from GFP-transgenic syngeneic C57B6/J mice as previously described (Mizumoto, Mizumoto et al. 2003). GFP-mNSCs were isolated at age P1 in order to achieve a primarily gliogenic cell phenotype, promoting differentiation of these NSCs into support cells and not neuronal subtypes (i.e., DAergic, serotonergic). $BDNF^{shRNA}$ GFP-mNSCs were generated as previously described, using lentiviral delivery and stable selection of a shRNA construct targeting murine BDNF (Blurton-Jones, Kitazawa et al. 2009). Twelve month old ASO and WT mice were randomly assigned to a treatment group and either vehicle or 50,000 mNSCs/site (1µl volume, 2 sites per hemisphere) were transplanted bilaterally into the dorsal striatum (Bregma +0.03 AP, ± 2.0 ML, -3.0 and -3.5 DV). mNSCs remained on ice for the duration of the transplantation procedure and retained 89-94% viability. Mice were anesthetized with isoflurane, placed in the stereotax and injected with either 100,000 mNSCs per site (or vehicle (1x HBSS with 20 ng/mL hEGF) as a control treatment using a 5 µL Hamilton microsyringe (30-gauge) and an injection rate of 0.5 µL/min. Cells were delivered at two DV sites (1µl/site) per hemisphere to facilitate distribution of mNSCs throughout the dorsal and ventral medial striatum. The needle was retained within the

injection site for 4 minutes before slowly removing the needle to reduce potential backflow of cells along the needle tract. For AAV experiments, AAV2-mCherry or AAV-mCherry-BDNF were injected bilaterally at the same striatal coordinates (1µl of 1.5 x10^{13} viral particles/ml; Vector Biolabs). Accurate injection to the targeted region was confirmed by visualization of the needle tract and GFP cells or mCherry within coronal brain sections.

Pharmacological Studies. Mice were administered intraperitoneal injections of the GLT-1 inhibitor dihydrokainic acid (DHK; 10 mg/kg/day; Tocris Bioscience, Briston, UK; (Gunduz, Oltulu et al. 2011, Gunduz, Oltulu et al. 2011). Mice recovered for 2 days following stereotactic surgery; thereafter, DHK was administered once daily until the time of sacrifice. Intraperitoneal α-methyl-p-tyrosine methyl ester hydrochloride (αMT; 100 mg/kg/day; Sigma Aldrich, St. Louis, MO, USA; (Kelly, Rubinstein et al. 1998, Sotnikova, Beaulieu et al. 2005, Rung, Rung et al. 2011) was administered daily beginning 10 days prior to sacrifice (i.e., during behavioral training and assessment). Assessment of safety αMT was conducted in our laboratory as described in SI Figure 3.

Cognitive and Motor Behavioral Timeline & Assessment. Thirty days following transplantation, behavioral assessments began lasting 10 days. On day 41, brains were harvested for histological and biochemical processing. All behavioral testing and analysis was performed blinded to treatment and genotype groups using an identification system decoded during statistical analysis. Cortical- and hippocampal-dependent memory tasks followed standard protocols for NOR and novel place recognition (NPR; (Bermudez-Rattoni, Okuda et al. 2005, Barker, Bird et al. 2007, Balderas, Rodriguez-Ortiz et al. 2008, McNulty, Barrett et al. 2012). Briefly, mice were allowed to explore the object-free recognition chamber with only bedding for 5 minutes, 3 consecutive days. On the 4th day, mice were trained for 10 minutes in the presence

of 2 identical objects. Twenty-four hours later, one object was replaced with a novel one (NOR), or one object was moved to a novel location in the chamber (NPR) and animals were allowed to explore for 5 minutes. Object exploration was analyzed as degree of discrimination between novel and familiar objects [$((Time_{novel}-Time_{familiar})/(Time_{novel}+Time_{familiar}))*100$]. Importantly, it was determined that mean distance traveled, mean ambulatory speed and time spent investigating objects during the training period were not altered by either genotype or treatment for any of the reported studies (**SI Figure 1**). Animals that lacked exploratory behavior (< 4 seconds total exploration) were excluded. Mice were next tested on pole descent, Rotarod and beam traversal tasks. For Rotarod, mice were trained for 5 consecutive trials at 12 rpm to stay on the fixed speed Rotarod for 2 min (Ugo Basile, Italy). Twenty-four hours later, mice are tested at 12 rpm for 2 min and latency to fall off of the rotating rod is measured. The pole test has been used previously to assess basal ganglia-related movement deficits in mice, finding that Parkinsonian mice display slower performance on this task than controls (Matsuura, Kabuto et al. 1997, Sedelis, Schwarting et al. 2001, Fernagut, Chalon et al. 2003, Fleming, Salcedo et al. 2004). Briefly, mice are placed head-up atop a vertical pinewood pole (50 cm high, 1 cm diameter), which is based in a cage of bedding and then the time required to rotate into a head down position and descend the pole is measured. Finally, mice were tested on the beam traversal challenge as modified from Fleming et al 2004. Mice were trained for 2 days to traverse a narrowing Plexiglas beam to reach their home cages. On day 3, a mesh grid was placed over the beam, and mice were videotaped traversing from base to apex. The number of total steps and foot-faults (forelimb slipping through the wire grid) was counted by a blinded observer from slow motion video.

Biochemical Analyses. Six weeks after transplantation, mice were sacrificed by Euthasol and transcardial perfusion with 0.01 M phosphate-buffered saline (PBS). The left side of the brain was flash frozen for subsequent biochemical analysis. The right hemisphere was post-fixed in 4% paraformaldehyde, and sectioned on a microtome (40 μm, coronal) for immunohistochemical analyses. Half brain dorsal striatum, were microdissected. Each region was then processed to isolate mRNA and protein via Trizol (Life Technologies, Inc., Carlsbad CA) extraction. Both soluble and insoluble (Sarkosyl soluble) protein fractions were collected. Protein concentrations were determined via Bradford assay and normalized samples compared via SDS-PAGE Western blot. Relative signal intensity of grayscale images were then be quantified by Image J and once all values were obtained sample identification was decoded.

Immunofluorescent Labeling. Fluorescent immunohistochemistry followed previously described protocols (Blurton-Jones, Kitazawa et al. 2009). Briefly, coronal brain sections were rinsed 3 times in 0.01 M PBS, then placed into blocking solution (0.01 M PBS+0.02% Tx100+5% Goat serum) for 1 hr at room temperature. Primary antibodies were then diluted in fresh blocking solution and applied overnight at 4^{o}C. Sections were then rinsed in PBS and incubated for 1 hr at room temperature in appropriate highly-cross absorbed Alexa Fluor secondary antibodies (Life Technology). Following 3 additional rinses, sections were mounted on slides and cover-slipped using Fluoromount G (Southern Biotech). The following primary antibodies were used: Dopaminergic antibodies: tyrosine hydroxylase (Millipore, #ab152), pTH ser31 (Cell Signaling, #3370), pTH ser19 (PhosphoSolutions, #p1580-19). Neurotrophin Antibodies: BDNF (Santa Cruz Biotech., # sc-546), TrkB (Cell Signaling, #4603), GDNF (Santa Cruz Biotech., #sc-328), phosphor-Erk1/2 (Cell Signaling, #9101). Glutamatergic Antibodies: GLT-1 (Abcam, #ab106289), VGLUT1 (Synaptic Systems, #135303), VGLUT2 (Synaptic

Systems, #135403), GLAST (Novus Biologicals, #NB100-1869), EAAC1 (Alpha Diagnostics, #EAAC11-A). Differentiation Antibodies: GFAP (Millipore, #MAB260), DCX (Abcam, #ab18723), Olig2 (Millipore, #MABN50).

Confocal Microscopy and Quantification. Sections were imaged in a blinded manner using an Olympus Fluoview FV1200 confocal microscope. For analysis of human α-synuclein inclusions, sections were double-labeled for human and endogenous mouse α-synuclein. Relative signal intensity of grayscale images were then be quantified by Image J and once all values were obtained sample coding was revealed.

Statistical Analysis. All animals were randomly assigned to treatment groups based only on wild-type or transgenic genotype and sex. Animal identification codes were randomly generated in order to keep the researcher blind to genotype and treatment throughout the behavioral testing, scoring, and statistical analysis. All statistical comparisons were performed using Statview 5 software. Comparisons between multiple groups utilized two-way analysis of variance (ANOVA) followed by Fisher's PLSD *post hoc* tests, with the exception of ASO-BKC studies which utilized one-way ANOVA due to the unmatched group design. Differences are considered significant when $p<0.05$ for both ANOVA and *post hoc* tests.

REFERENCES

Amschl, D., J. Neddens, D. Havas, S. Flunkert, R. Rabl, H. Romer, E. Rockenstein, E. Masliah, M. Windisch and B. Hutter-Paier (2013). "Time course and progression of wild type alpha-synuclein accumulation in a transgenic mouse model." BMC Neurosci **14**: 6.

Balderas, I., C. J. Rodriguez-Ortiz, P. Salgado-Tonda, J. Chavez-Hurtado, J. L. McGaugh and F. Bermudez-Rattoni (2008). "The consolidation of object and context recognition memory involve different regions of the temporal lobe." Learn Mem **15**(9): 618-624.

Barker, G. R., F. Bird, V. Alexander and E. C. Warburton (2007). "Recognition memory for objects, place, and temporal order: a disconnection analysis of the role of the medial prefrontal cortex and perirhinal cortex." J Neurosci **27**(11): 2948-2957.
Bermudez-Rattoni, F., S. Okuda, B. Roozendaal and J. L. McGaugh (2005). "Insular cortex is involved in consolidation of object recognition memory." Learn Mem **12**(5): 447-449.
Blurton-Jones, M., M. Kitazawa, H. Martinez-Coria, N. A. Castello, F. J. Muller, J. F. Loring, T. R. Yamasaki, W. W. Poon, K. N. Green and F. M. LaFerla (2009). "Neural stem cells improve cognition via BDNF in a transgenic model of Alzheimer disease." Proc Natl Acad Sci U S A **106**(32): 13594-13599.
Fernagut, P. O., S. Chalon, E. Diguet, D. Guilloteau, F. Tison and M. Jaber (2003). "Motor behaviour deficits and their histopathological and functional correlates in the nigrostriatal system of dopamine transporter knockout mice." Neuroscience **116**(4): 1123-1130.
Fleming, S. M., J. Salcedo, P. O. Fernagut, E. Rockenstein, E. Masliah, M. S. Levine and M. F. Chesselet (2004). "Early and progressive sensorimotor anomalies in mice overexpressing wild-type human alpha-synuclein." J Neurosci **24**(42): 9434-9440.
Gunduz, O., C. Oltulu, D. Buldum, R. Guven and A. Ulugol (2011). "Anti-allodynic and anti-hyperalgesic effects of ceftriaxone in streptozocin-induced diabetic rats." Neurosci Lett **491**(1): 23-25.
Gunduz, O., C. Oltulu and A. Ulugol (2011). "Role of GLT-1 transporter activation in prevention of cannabinoid tolerance by the beta-lactam antibiotic, ceftriaxone, in mice." Pharmacol Biochem Behav **99**(1): 100-103.
Kelly, M. A., M. Rubinstein, T. J. Phillips, C. N. Lessov, S. Burkhart-Kasch, G. Zhang, J. R. Bunzow, Y. Fang, G. A. Gerhardt, D. K. Grandy and M. J. Low (1998). "Locomotor activity in D2 dopamine receptor-deficient mice is determined by gene dosage, genetic background, and developmental adaptations." J Neurosci **18**(9): 3470-3479.
Masliah, E., E. Rockenstein, I. Veinbergs, M. Mallory, M. Hashimoto, A. Takeda, Y. Sagara, A. Sisk and L. Mucke (2000). "Dopaminergic loss and inclusion body formation in alpha-synuclein mice: implications for neurodegenerative disorders." Science **287**(5456): 1265-1269.
Matsuura, K., H. Kabuto, H. Makino and N. Ogawa (1997). "Pole test is a useful method for evaluating the mouse movement disorder caused by striatal dopamine depletion." J Neurosci Methods **73**(1): 45-48.
McNulty, S. E., R. M. Barrett, A. Vogel-Ciernia, M. Malvaez, N. Hernandez, M. F. Davatolhagh, D. P. Matheos, A. Schiffman and M. A. Wood (2012). "Differential roles for Nr4a1 and Nr4a2 in object location vs. object recognition long-term memory." Learn Mem **19**(12): 588-592.
Mizumoto, H., K. Mizumoto, M. A. Shatos, H. Klassen and M. J. Young (2003). "Retinal transplantation of neural progenitor cells derived from the brain of GFP transgenic mice." Vision Res **43**(16): 1699-1708.
Rung, J. P., E. Rung, A. M. Johansson, K. Svensson, A. Carlsson and M. L. Carlsson (2011). "Effects of the dopamine stabilizers (S)-(-)-OSU6162 and ACR16 on prolactin secretion in drug-naive and monoamine-depleted rats." Naunyn Schmiedebergs Arch Pharmacol **384**(1): 39-45.
Sedelis, M., R. K. Schwarting and J. P. Huston (2001). "Behavioral phenotyping of the MPTP mouse model of Parkinson's disease." Behav Brain Res **125**(1-2): 109-125.
Sotnikova, T. D., J. M. Beaulieu, L. S. Barak, W. C. Wetsel, M. G. Caron and R. R. Gainetdinov (2005). "Dopamine-independent locomotor actions of amphetamines in a novel acute mouse model of Parkinson disease." PLoS Biol **3**(8): e271.